Chemical trend of a Cu impurity in Zn chalcogenides

Yang Yang,[1] Peng Zhang,[2,*] Jingxiu Yang,[3,†] and Su-Huai Wei[1,‡]
[1]Beijing Advanced Innovation Center for Materials Genome Engineering, Beijing Computational Science Research Center, Beijing, 100193, China
[2]College of Physics and Optoelectronic Engineering, Shenzhen University, Shenzhen, Guangdong 518060, China
[3]School of Materials Science and Engineering, Jilin Jianzhu University, Changchun 130118, China

(Received 13 February 2020; revised manuscript received 9 April 2020; accepted 16 April 2020; published 1 May 2020)

Cu is usually considered as an effective dopant to introduce shallow acceptors in Zn chalcogenides because it is on the left-hand side of Zn in the Periodic Table. Here, using first-principles calculations based on the hybrid functional with spin polarization, we show that contrary to the common expectation, Cu substituting Zn (Cu_{Zn}) in bulk Zn chalcogenides actually generates rather deep acceptor levels in ZnO, ZnS, and ZnSe, i.e., 2.91, 1.03, and 0.53 eV above the valence-band maximum (VBM), respectively, except in ZnTe (0.13 eV). More interestingly, the absolute Cu impurity energy level does not follow the variation of the VBM, decreasing from ZnTe to ZnSe to ZnS to ZnO, instead, it is the highest in ZnO. The abnormal behavior of Cu_{Zn} in ZnO is attributed to the fact that, due to the very low O 2p-orbital energy, the Cu_{Zn} defect wave function has dominantly localized the Cu 3d-orbital component, whereas in other Zn chalcogenides, anion p states are dominant. The localized Cu 3d state leads to the enhanced exchange energy that elevates the acceptor level, which explains why the Cu impurity level is abnormally deep in ZnO. This finding provides insight in designing shallow acceptor levels in II–VI semiconductors.

DOI: 10.1103/PhysRevB.101.174101

I. INTRODUCTION

Zinc chalcogenides (ZnX, X = O, S, Se, and Te) are important semiconductors with direct band gaps covering a large range of the spectrum, and, thus, have a wide range of applications in optoelectronics and electroluminescence [1–11]. ZnSe and ZnTe are important materials for window layers in thin-film solar cells and were used to form green light-emitting diodes and lasers [12–16]. ZnO and ZnS have also been considered as cost-effective electroluminescent materials to replace group-III nitrides if p-type doping issues can be resolved. Given that the performance of ZnX-based devices depends critically on their defect properties, it is necessary to understand the electronic structure of the impurities in ZnX.

Cu, which is on the left-hand side of Zn in the Periodic Table, is expected to be an effective p-type dopant in ZnX when Cu substitutes on the Zn site, Cu_{Zn}, because Cu and Zn have small size mismatch and similar valence electron configurations. Indeed, Cu acts as a shallow dopant in ZnTe with the acceptor level at about 0.15 eV above the valence-band maximum (VBM) by the electrical transport measurements [17]. The Cu dopant levels in ZnSe and ZnS become deeper relative to the VBM, which is expected as the VBM moves down in energy from ZnTe to ZnSe and to ZnS [18,19]. Although there are experimental reports demonstrating that the p-type conductivity can be realized in ZnS, ZnSe, and ZnTe by Cu doping [20–22], the realization of p-type conductivity in Cu-doped ZnO has not been reported, which implies that the intrinsic property of the Cu dopant in ZnO might differ substantially from other ZnX's.

Previous density functional theory calculations within the local density approximation (LDA) showed that, unlike group-IA elements, Cu prefers to substitute Zn in ZnO [6]. The calculated transition energy level of Cu_{Zn} is at 0.7 eV above the VBM. On the other hand, the experimental measurements *via* different techniques, such as optical and electrical spectroscopies [23], admittance spectroscopy [24], and electron paramagnetic resonance [25], showed that Cu_{Zn} in ZnO yields an acceptor level of ~0.2 eV below the conduction-band minimum (CBM), i.e., 3.2 eV above the VBM, which is much deeper than the LDA prediction. This inconsistency between the LDA prediction and the experiments should be largely ascribed to the well-known underestimation of the band gap by the LDA method due to the lack of correction on the self-interaction error [26]. In fact, a recent theoretical calculation with a hybrid functional revealed a rather deep acceptor level of Cu_{Zn} in ZnO (3.27 eV above the VBM) [27], which is in good agreement with the experimental observation. However, the physical origin of this deep acceptor level of Cu_{Zn} in ZnO has not been explained. Moreover, to get more comprehensive understanding on the defect properties in ZnX and for the future design of ZnX-based optoelectronic devices, it is also important to reveal the general chemical trend of Cu doping in these systems as the anion changes from O to S to Se and to Te.

In this paper, using first-principles calculations with the hybrid functional, we systematically study the defect

*pengzhang@szu.edu.cn
†yangjingxiu@jlju.edu.cn
‡suhuaiwei@csrc.ac.cn

 ©2020 American Physical Society

properties of Cu_{Zn} in the series of Zn*X* (X = O, S, Se, and Te). Our results indicate that the acceptor level of Cu_{Zn} in Zn*X* changes profoundly as the anion changes from O to S to Se and to Te. In ZnO, we find that Cu_{Zn} generates a rather deep acceptor level of 2.91 eV above the VBM, i.e., 0.16 eV below the calculated CBM, which is unusually deep by the common expectation, but consistent with experimental observations. More interestingly, the absolute Cu impurity energy level does not follow the variation of the VBM, decreasing from ZnTe to ZnSe to ZnS to ZnO, instead, it is the highest in ZnO. This phenomenon can be ascribed to the fact that because the VBM of the ZnO is very low in energy, the defect states of Cu_{Zn} in ZnO are dominated by localized Cu 3*d* orbitals with some hybridization with O 2*p* orbitals, leading to significant exchange energy that elevates the acceptor level. On the contrary, for the other Zn*X*, the predominant character of the defect states of Cu_{Zn} is found to be more and more anion *p* like from ZnS to ZnSe to ZnTe. As a consequence, the spatial distribution of the defect states become more delocalized, which reduces the exchange energy and lowers the acceptor level. Thus, our studies imply that it is important to adjust the relative energy of dopant versus host element orbitals to realize the effective *p*-type doping in II–IV semiconductors.

II. COMPUTATIONAL METHOD

Our spin-polarized calculations are carried out by using the projector augmented wave method with the Heyd-Scuseria-Ernzerhof hybrid functional [28,29] as implemented in the Vienna *ab initio* simulation package code [30]. To be consistent with the experimental band gaps of Zn*X*, the mixing parameter for the Hartree-Fock exchange term is set to be 0.33. The calculated band gaps for the zinc-blende ZnO, ZnS, ZnSe, and ZnTe are 3.07, 3.74, 2.79, and 2.41 eV, respectively, in reasonably good agreement with the experimental values of 3.27, 3.78, 2.82, and 2.39 eV [31,32]. Moreover, the formation energies of ZnO, ZnS, ZnSe, and ZnTe are found to be −3.66, −1.98, −1.77, and −1.30 eV, respectively, which also agree with the experimental results of −3.60, −2.09, −1.83, and −1.23 eV [33]. For the defect calculations, a supercell containing 64 atoms with one Cu substituting on Zn is adopted. The wave functions are expanded by using the plane waves up to a kinetic-energy cutoff of 400 eV, and a Γ-centered $3 \times 3 \times 3$ k mesh is used for the Brillouin-zone integration. During the relaxation, the lattice constants are fixed at their bulk equilibrium values, whereas all the atomic coordinates are fully relaxed until the Hellman-Feynman force on each atom is less than 0.01 eV/Å. To compare the defect levels of Cu_{Zn}, we need to align the VBM of different Zn*X* compounds [34,35]. The valence-band offset of two compounds can be calculated by

$$\Delta E_v(AX/BY) = \Delta E_{v,C'}(BY) - \Delta E_{v,C}(AX) + \Delta E_{C,C'}(AX/BY), \quad (1)$$

where $\Delta E_{v,C}(AX) = E_v(AX) - E_C(AX)$ [the same for $\Delta E_{v,C'}(BY)$] is the energy difference between the VBM and the core level for the compound AX, and $\Delta E_{C,C'}(AX/BY) = E_{C'}(BY) - E_C(AY)$ is the energy difference between the core levels of compounds AX and BY, calculated in an AX/BY heterostructure. The more detailed calculation method can be found in Refs. [36–38].

TABLE I. The chemical potential range for Cu doping in Zn*X* under the anion-rich condition.

	μ_{anion}	μ_{Zn}	μ_{Cu}
ZnO	0	−3.66	<−1.51
ZnS	0	−1.98	<−0.56
ZnSe	0	−1.77	<−0.60
ZnTe	0	−1.30	<−0.44

For defects in different charge states, their formation energies can be calculated by using the well-established formalism [39],

$$\Delta H_f(\alpha, q) = \Delta E(\alpha, q) + \sum n_i \mu_i + qE_F \,, \quad (2)$$

where $\Delta E(\alpha, q) = E(\alpha, q) - E(\text{host}) + \sum n_i E(i) + q\varepsilon_{\text{VBM}}$. Here, $E(\text{host})$ is the total energy of the supercell, and $E(\alpha, q)$ is the total energy of the same supercell but with a defect α. n_i is the number of elements, and q is the number of electrons transferred from the supercell to the reservoirs in forming the defect cells. ε_{VBM} is the VBM energy of the host, and E_F is the Fermi energy referenced to ε_{VBM}. μ_i is the chemical potential of element i referenced to $E(i)$, the total energy of the bulk element i. The transition energy level with respect to the VBM is given by

$$\varepsilon(0/q) = \left[\varepsilon_D^{\Gamma}(0) - \varepsilon_{\text{VBM}}^{\Gamma}(\text{host})\right] + \left\{E(\alpha, q) - \left[E(\alpha, 0) - q\varepsilon_D^{\text{k}}(0)\right]\right\}/(-q). \quad (3)$$

The first term on the right-hand side of Eq. (3) gives the single-electron energy level of the defect at the Γ point, and the second term determines the relaxation energy U of the charged defects calculated at the special k points, which is the extra cost of energy by moving charge q from the VBM of the host to the defect level.

From Eq. (2), we can see that the calculated formation energy of a defect relies on the choice of chemical potentials. For example, in the case of Cu_{Zn} in ZnO, the chemical potential range varies according to the formation enthalpy of ZnO,

$$\mu_{\text{Zn}} + \mu_{\text{O}} = \Delta H_{\text{f}}(\text{ZnO}) = -3.66\,\text{eV}. \quad (4)$$

Furthermore, the chemical potentials are limited by the formation of elementary dopants and host elements, i.e., $\mu_{\text{Zn}} < \mu(\text{Zn}) = 0$, $\mu_{\text{O}} < \mu(\text{O}) = 0$, and $\mu_{\text{Cu}} < \mu(\text{Cu}) = 0$. Finally, to avoid the formation of possible secondary phases, several additional constraints of chemical potentials should be also satisfied

$$\mu_{\text{Cu}} + \mu_{\text{O}} < \Delta H_{\text{f}}(\text{CuO}) = -1.51\,\text{eV}, \quad (5)$$

$$2\mu_{\text{Cu}} + \mu_{\text{O}} < \Delta H_{\text{f}}(\text{CuO}) = -1.60\,\text{eV}. \quad (6)$$

By taking all these constraints into account, the chemical potential range can be identified. The chemical potential ranges for Cu doping in Zn*X* under the anion-rich condition are summarized in Table I.

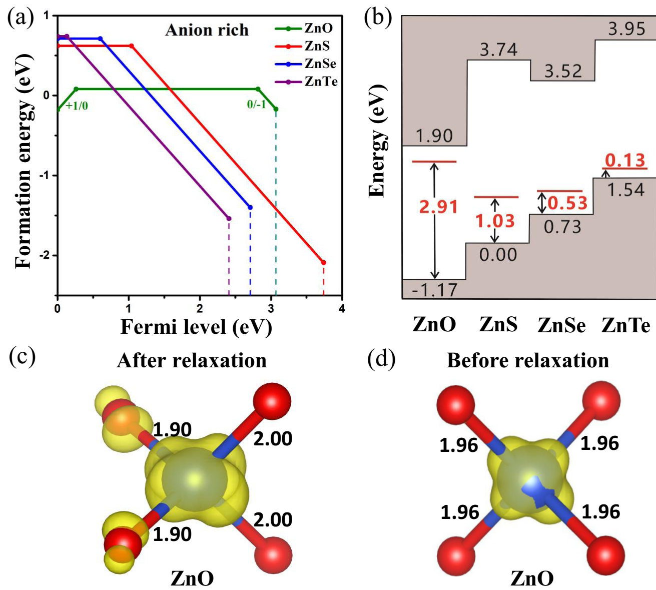

FIG. 1. (a) Calculated formation energy of Cu_{Zn} as a function of the Fermi level in Zn chalcogenides under an anion-rich condition. The VBMs of ZnX are all set as zero, and the CBMs are represented by the dashed line with the corresponding color for the semiconductors. (b) Calculated valence-band offsets and (0/−) acceptor levels in Zn chalcogenides. By setting the VBM of ZnS as zero, the VBMs in ZnO, ZnSe, and ZnTe are at −1.17, 0.73, and 1.54 eV, respectively. (c) and (d) The structure of Cu_{Zn} in ZnO after and before ionic relaxation. The blue and red spheres represent the Cu and O atoms, respectively. The yellow isosurface represents the charge-density distribution of the Cu_{Zn} defect level.

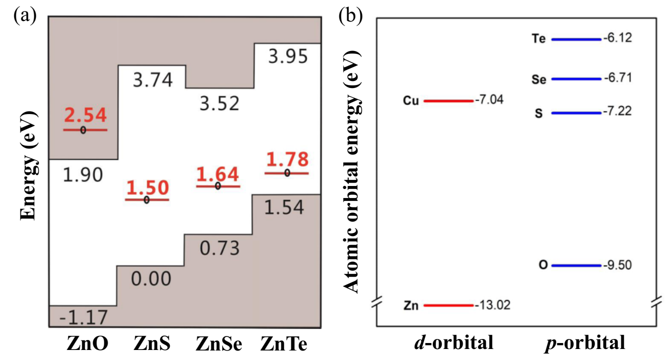

FIG. 2. (a) The single-electron energy level of Cu_{Zn} in Zn chalcogenides. The red line with a circle indicates an empty (hole) state within the spin-down channel. The energy zero is set at the VBM of ZnS. (b) The calculated atomic energy levels of p and d orbitals of the relevant elements in this paper with hybrid functional and spin-orbital couplings. The energy zero is the potential at infinity.

III. RESULTS AND DISCUSSION

Figure 1(a) shows the calculated formation energies of Cu_{Zn} in ZnX as a function of the Fermi energy under the anion-rich condition. The formation energies of neutral Cu_{Zn} under the anion-rich condition are calculated to be 0.08, 0.64, 0.71, and 0.74 eV in ZnO, ZnS, ZnSe, and ZnTe, respectively. Figure 1(b) shows the calculated (0/−1) transition energy levels of Cu_{Zn} in ZnS, ZnSe, and ZnTe are 1.03, 0.53, and 0.13 eV above the VBM, respectively, in good agreement with their experimental ionization energies of 1.10 [18,40], 0.65 [41], and 0.15 eV [17]. Whereas in ZnO, we find that Cu_{Zn} can act as either an acceptor or a donor, depending on the Fermi energy, with the corresponding (0/−) and (+/0) transition energy levels located at 2.91 and 0.39 eV above the VBM, respectively. This result agrees with the previous theoretical calculations [27] and experimental measurements which revealed that the acceptor level of Cu_{Zn} in ZnO is rather deep (∼0.2 eV below the CBM) [23–25]. We have also tested the convergence of the supercell size using a 512-atom cell and find that the calculated transition energy levels are converged to be within 0.16 eV and do not change the chemical trend. From these calculations, we can clearly see that the property of Cu doping in ZnO differs substantially from that in other ZnX.

To understand the chemical trend of Cu doping in ZnX, we next turn to examine the structural and electronic properties of Cu_{Zn} in more detail. It has been realized that the local structural distortion associated with the variation of the charge state of a defect can significantly alter its transition energy level. For example, the unexpected deep acceptor level found for Be substituting on Ga site (Be_{Ga}) in GaN has been ascribed to the different defect charge distributions and associated structural distortion as it changes from the ground to the excited states [42–44]. For Cu doping in ZnX, the similar local structural distortion may also occur. Indeed, when Cu substitutes Zn in ZnO, one hole is introduced into the originally closed 3d shell of Cu, which leads to a T_d to D_{2d} Jahn-Teller-like structural distortion around the defect as illustrated in Fig. 1(c). As a consequence, the resultant energy splitting of the defect states of Cu_{Zn} would elevate its (0/−1) transition energy level. To estimate the impact of this Jahn-Teller distortion, we intentionally froze the structural relaxation when Cu is doped into ZnO as shown in Fig. 1(d). The calculated single electron level using this unrelaxed structure is 3.10 eV above the VBM, quite close to the value (3.16 eV) obtained with the fully relaxed structure. This result indicates that the effect of local structural distortion on the acceptor level of Cu_{Zn} in ZnO is quite limited. The Jahn-Teller-like structural distortion is weaker in ZnS, and no such Jahn-Teller-like structural distortion is found in ZnSe and ZnTe. Therefore, we have to look for other reasons that are responsible for the extremely deep Cu_{Zn} level in ZnO.

To further investigate the issue, we show in Fig. 2(a) the calculated band alignments and absolute single-electron energy levels of Cu_{Zn} in ZnX. For ZnX with the zinc-blende structure, the VBM is mainly composed of anion p orbitals, whereas the CBM has mostly the Zn s and anion s characters. The projected density of states (PDOS) are shown in Fig. 3. Both the single-electron energy levels and the (P)DOS are for neutral Cu_{Zn}. As a consequence, the VBM of ZnX is found to increase monotonically with the increased anion p orbital energy from O to S to Se and to Te as illustrated in Figs. 2(a) and 2(b). The atomic levels in Fig. 2(b) are obtained by calculating a $30\times30\times30$ Å^3 supercell containing one atom in this paper. As Cu substitutes Zn in ZnX, one hole is introduced into the system since Cu has one electron less than Zn, creating an empty (hole) state presented by the red

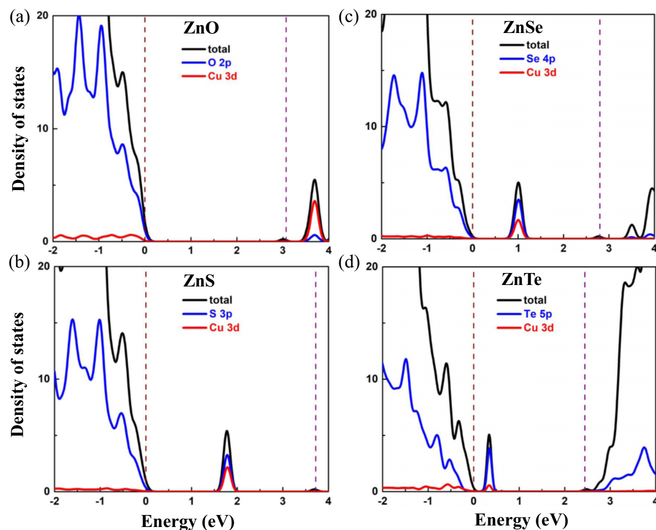

FIG. 3. The total and the projected density of states of the anion p orbital, Cu $3d$ orbital of the Cu_{Zn}^{0} defect state in Zn chalcogenides. The Fermi level is set at zero at the VBMs and denoted by the brown dashed lines, and the CBMs are denoted by the purple dashed lines.

line in Fig. 2(a). We note that an energy splitting (ΔE_{split}) between this hole state and the host band exists for all the ZnX compounds, exhibiting a Mott-insulator-like character of their electronic structures. From ZnTe to ZnSe and to ZnS, ΔE_{split} is found to increase gradually due to the lowering of the VBM energy. However, generally, it can be seen that the single-electron energy levels of the hole state are still close to the VBM, presenting a typical p-type doping character of Cu_{Zn} in these ZnX's. For ZnO, on the other hand, we find that ΔE_{split} becomes abnormally large, shifting the hole state to be above the CBM as shown in Fig. 2(a). This indicates that the large ΔE_{split} and, thus, the high single-electron energy level of the hole state, is responsible for the deep acceptor level of Cu_{Zn} found for ZnO.

Figure 3 plots the total density of states and the PDOS of Cu_{Zn} in ZnX. We note that the defect states associated with Cu_{Zn} are mainly constructed by the hybridization between Cu $3d$ and anion p orbitals as shown in Fig. 3. For ZnO [Fig. 3(a)] because of the very low O $2p$ orbital energy [Fig. 2(b)], the defect state is dominated by the Cu $3d$ orbital with the contribution of ~79%, compared to the O $2p$-orbital contribution of ~21%. This dominant Cu $3d$ character of the defect states would induce a very large exchange splitting between the occupied (electron) and the empty (hole) levels due to the localized nature of its wave function, giving rise to the promoted hole state above the CBM as shown in Fig. 2(a). On the other hand, for other ZnX's [Figs. 3(b)–3(d)] because they have high X p-orbital energy [Fig. 2(b)], the composition of the defect states changes significantly and their dominant character changed from Cu $3d$ to anion p like. For example, comparing ZnTe with ZnO, we find that the contribution of Cu $3d$ orbitals to the defect states decreases from 79% to 11%, whereas that of anion p orbitals increases from 21% to 89%. As a result, the spatial distribution of the defect-state wave function becomes profoundly extended in ZnS, ZnSe, and ZnTe, compared to that in ZnO, which would reduce the exchange splitting between the electron and the hole states as shown in Fig. 2(a). The abrupt change in the character of the defect states of Cu_{Zn} from ZnO to other ZnX's, thus, is responsible for the nonmonotonic change in Cu_{Zn} from ZnO to other ZnX's.

IV. CONCLUSION

To summarize, based on the first-principles hybrid functional calculations, we systematically investigate the chemical trend of Cu doping in ZnX. We find that the acceptor level of Cu_{Zn} becomes shallower as the anion atomic number increases from ZnS to ZnSe to ZnTe (i.e., 1.03, 0.53, and 0.13 eV above the VBM, respectively) as expected, but the Cu_{Zn} acceptor level in ZnO is unusually high at 2.91 eV above the VBM, even though the VBM energy of ZnO is only 1.2 eV lower than that of ZnS. We show that the unusually deep acceptor level of Cu_{Zn} in ZnO is due to its dominantly localized Cu $3d$-orbital component, which leads to a very large exchange splitting between the electron and the hole levels, thus, elevating the acceptor level of the defect. On the contrary, for the other ZnX's, the defect states are predominantly anion p like and, therefore, less localized. This significantly reduces the exchange splitting of the defect states and, thus, leads to relatively shallow acceptor levels of Cu_{Zn} in these ZnX's. The chemical trend of Cu doping in ZnX revealed in this paper, thus, provides insight and a theoretical guideline for the future design of shallow acceptors in II–VI semiconductors.

ACKNOWLEDGMENTS

This work was supported by the Science Challenge Project under Grant No. TZ2016003, the National Key Research and Development Program of China (Grant No. 2016YFB0700700), and the National Nature Science Foundation of China (Grants No. 51672023, No. 11634003, No. U1930402, No. 61827815, and No. 11774239). The computation was supported by the Beijing Computational Science Research Center (CSRC).

[1] Y. Yan, S. B. Zhang, and S. T. Pantelides, Phys. Rev. Lett. **86**, 5723 (2001).
[2] S. Limpijumnong, S. B. Zhang, S.-H. Wei, and C. H. Park, Phys. Rev. Lett. **92**, 155504 (2004).
[3] D. C. Look, D. C. Reynolds, C. W. Litton, R. L. Jones, D. B. Eason, and G. Cantwell, Appl. Phys. Lett. **81**, 1830 (2002).
[4] S. B. Zhang, S.-H. Wei, and A. Zunger, Phys. Rev. B **63**, 075205 (2001).
[5] C. H. Park, S. B. Zhang, and S.-H. Wei, Phys. Rev. B **66**, 073202 (2002).
[6] Y. Yan, M. M. Al-Jassim, and S. H. Wei, Appl. Phys. Lett. **89**, 181912 (2006).

[7] K. S. Ahn, T. Deutsch, Y. Yan, C. S. Jiang, C. L. Perkins, and J. Turner, J. Appl. Phys. **102**, 023517 (2007).
[8] M. Suja, S. B. Bashar, M. M. Morshed, and J. Liu, ACS Appl. Mater. Inter. **7**, 8894 (2015).
[9] S. Muthukumaran and M. Ashok kumar, Mater. Lett. **93**, 223 (2013).
[10] G. K. Mani and J. B. B. Rayappan, J. Alloys Compd. **582**, 414 (2014).
[11] R. Dingle, Phys. Rev. Lett. **23**, 579 (1969).
[12] Y. Fan, J. Han, L. He, J. Saraie, R. L. Gunshor, M. Hagerott, H. Jeon, A. V. Nurmikko, G. C. Hua, and N. Otsuka, Appl. Phys. Lett. **61**, 3160 (1992).
[13] J. Ren, K. A. Bowers, B. Sneed, D. L. Dreifus, J. W. Cook, Jr., J. F. Schetzina, and R. M. Kolbas, Appl. Phys. Lett. **57**, 1901 (1990).
[14] M. A. Haase, J. Qiu, J. M. DePuydt, and H. Cheng, Appl. Phys. Lett. **59**, 1272 (1991).
[15] Q. Wu, M. Litz, and X. C. Zhang, Appl. Phys. Lett. **68**, 2924 (1996).
[16] K. Sato, M. Hanafusa, A. Noda, A. Arakawa, M. Uchida, T. Asahi, and O. Oda, J. Cryst. Growth **214**, 1080 (2000).
[17] M. Aven and B. Segall, Phys. Rev. **130**, 81 (1962).
[18] S. Ummartyotin, N. Bunnak, and H. Manuspiya, Solid State Sci. **14**, 299–304 (2012).
[19] M. C. Tamargo, *II-VI Semiconductor Materials and their Applications* (CRC, New York, 2002).
[20] D. E. Ortíz-Ramos, L. A. González, and R. Ramirez-Bon, Mater. Lett. **124**, 267 (2014).
[21] M. Orita, T. Narushima, and H. Yanagita, Jpn. J. Appl. Phys., Part 2 **46**, L976 (2007).
[22] V. S. John, T. Mahalingam, and J. P. Chu, Solid-State Electron. **49**, 3 (2005).
[23] G. Muller, Phys. Status Solidi B **76**, 525 (1976).
[24] Y. Kanai, J. Appl. Phys. **30**, 703 (1991).
[25] R. E. Dietz, H. Kamimura, M. D. Sturge, and A. Yariv, Phys. Rev. **132**, 1559 (1963).
[26] C. Freysoldt, B. Grabowski, T. Hickel, J. Neugebauer, G. Kresse, A. Janotti, and C. G. Van de Walle, Rev. Mod. Phys. **86**, 253 (2014).
[27] J. L. Lyons, A. Alkauskas, A. Janotti, and C. G. Van de Walle, Appl. Phys. Lett. **111**, 042101 (2017).
[28] J. Heyd, G. E. Scuseria, and M. Ernzerhof, J. Chem. Phys. **118**, 8207 (2003).
[29] J. P. Perdew, K. Burke, and M. Ernzerhof, Phys. Rev. Lett. **77**, 3865 (1996).
[30] G. Kresse and J. Furthmuller, Phys. Rev. B **54**, 11169 (1996).
[31] H. Dixit, R. Saniz, D. Lamoen, and B. Partoens, J. Phys.: Condens. Matter **22**, 125505 (2012).
[32] O. Madelung, *Semiconductors: Data Handbook* (Springer, Berlin, 2012).
[33] A. Nasar and M. Shamsuddin, Thermochim. Acta **205**, 157 (1992).
[34] J. M. Langer and H. Heinrich, Phys. Rev. Lett. **55**, 1414 (1985).
[35] M. J. Caldas, A. Fazzio, and A. Zunger, Appl. Phys. Lett. **45**, 671 (1984).
[36] S. H. Wei and A. Zunger, Phys. Rev. Lett. **59**, 144 (1987).
[37] S. H. Wei and A. Zunger, Appl. Phys. Lett. **72**, 2011 (1998).
[38] A. Franceschetti, S. H. Wei, and A. Zunger, Phys. Rev. B **50**, 17797 (1994).
[39] S. H. Wei, Comput. Mater. Sci. **30**, 337 (2004).
[40] B. B. Srivastava, S. Jana, and N. Pradhan, J. Am. Chem. Soc. **133**, 1007 (2010).
[41] R. N. Bhargava, J. Cryst. Growth **59**, 15 (1982).
[42] X. Cai, J. Yang, P. Zhang, and S.-H. Wei, Phys. Rev. Appl. **11**, 034019 (2019).
[43] S. Lany and A. Zunger, Appl. Phys. Lett. **96**, 142114 (2010).
[44] J. L. Lyons, A. Janotti, and C. G. Van de Walle, Jpn. J. Appl. Phys. **52**, 08JJ04 (2013).